Archival Report

Biological Psychiatry: CNNI

Strategic Infarct Locations for Poststroke Depressive Symptoms: A Lesion- and Disconnection-Symptom Mapping Study

Nick A. Weaver, Jae-Sung Lim, Janniek Schilderinck, Geert Jan Biessels, Yeonwook Kang, Beom Joon Kim, Hugo J. Kuijf, Byung-Chul Lee, Keon-Joo Lee, Kyung-Ho Yu, Hee-Joon Bae, and J. Matthijs Biesbroek

ABSTRACT

BACKGROUND: Depression is the most common neuropsychiatric complication after stroke. Infarct location is associated with poststroke depressive symptoms (PSDS), but it remains debated which brain structures are critically involved. We performed a large-scale lesion-symptom mapping study to identify infarct locations and white matter disconnections associated with PSDS.

METHODS: We included 553 patients (mean [SD] age = 69 [11] years, 42% female) with acute ischemic stroke. PSDS were measured using the 30-item Geriatric Depression Scale. Multivariable support vector regression (SVR)–based analyses were performed both at the level of individual voxels (voxel-based lesion-symptom mapping) and at predefined regions of interest to relate infarct location to PSDS. We externally validated our findings in an independent stroke cohort (N = 459). Finally, disconnectome-based analyses were performed using SVR voxel-based lesion-symptom mapping, in which white matter fibers disconnected by the infarct were analyzed instead of the infarct itself.

RESULTS: Infarcts in the right amygdala, right hippocampus, and right pallidum were consistently associated with PSDS (permutation-based $p < .05$) in SVR voxel-based lesion-symptom mapping and SVR region-of-interest analyses. External validation confirmed the association between infarcts in the right amygdala and pallidum, but not the right hippocampus, and PSDS. Disconnectome-based analyses revealed that disconnections in the right parahippocampal white matter, right thalamus and pallidum, and right anterior thalamic radiation were significantly associated (permutation-based $p < .05$) with PSDS.

CONCLUSIONS: Infarcts in the right amygdala and pallidum and disconnections of right limbic and frontal cortico-basal ganglia-thalamic circuits are associated with PSDS. Our findings provide a comprehensive and integrative picture of strategic infarct locations for PSDS and shed new light on pathophysiological mechanisms of depression after stroke.

https://doi.org/10.1016/j.bpsc.2021.09.002

Depression is the most common neuropsychiatric complication after stroke, affecting approximately one third of stroke survivors (1). Individuals with poststroke depression are at a higher risk of functional impairment, reduced quality of life, and increased mortality (2). Despite its high prevalence and debilitating impact on patients, the pathophysiology of poststroke depression remains poorly understood (3). Better understanding the pathophysiology is a critical step toward developing targeted prevention and treatment strategies, as was emphasized in a recent statement from the American Heart Association and American Stroke Association (3).

Infarct location has been identified as a contributor to poststroke depressive symptoms (PSDS), yet it remains debated which brain structures are critically involved. Numerous reviews on this topic have been published in the past 2 decades, but results are inconsistent (Table S1). The most recent systematic review and meta-analysis to date (covering literature up to 2016) found that infarcts in frontal and subcortical locations as well as in the basal ganglia were significantly associated with PSDS (4). However, many original studies considered only relatively crude spatial characteristics (e.g., hemispheric lateralization or frontal lobe involvement) (4,5). In the past decade, several studies have applied lesion-symptom mapping techniques to analyze the relationship between infarct location and depressive symptoms at a more detailed spatial resolution, usually at the level of individual brain voxels (6–10). Previous studies found significant associations for infarcts in the left dorsolateral prefrontal cortex (7), left ventrolateral prefrontal cortex (11), and posterior cerebellum (8), while three studies found no significant associations

ISSN: 2451-9022

(6,9,10). The lack of consistent evidence may be due to modest sample sizes in individual studies (i.e., largest single-center sample was N = 270) or specific inclusion criteria [e.g., only left hemispheric infarcts (7) or isolated cerebellar infarcts (8)], both resulting in limited lesion coverage of the brain. Lesion coverage is important in lesion-symptom mapping studies because if an anatomical structure is not damaged in a sufficient number of patients, potential structure-function relationships will not be detected. Of note, the largest lesion-symptom mapping study on PSDS to date (N = 461) largely consisted of a mixed population, including individuals with traumatic brain injury and intracerebral hemorrhages and only approximately 40% with ischemic stroke (9). In light of differences in disease mechanisms, this may have affected the results. A large-scale study with a homogeneous population could overcome these challenges.

Notably, a recent study proposed that disconnections caused by an infarct, rather than the location of the infarct itself, might also be related to depressive symptoms. In a combined sample from 5 datasets with different lesion etiologies, no specific lesion locations were associated with depressive symptoms, yet when functional disconnections (as identified using a normative functional connectome dataset) caused by each lesion were analyzed, robust associations with functional disconnection of the left dorsolateral prefrontal cortex were found (9).

In this large-scale study, we aimed to identify infarct locations associated with PSDS using multivariable lesion-symptom mapping, which we subsequently validated in an independent stroke cohort. Additionally, building on emerging evidence, we performed structural disconnection-symptom mapping analyses using the same multivariable analysis approach.

METHODS AND MATERIALS

Study Population

Patients were retrospectively selected from the Bundang Vascular Cognitive Impairment (VCI) cohort, which consisted of patients admitted to Seoul National University Bundang Hospital, Republic of Korea, registered in a prospective stroke registry database (12). For cohort inclusion, patients required hospital admission with acute ischemic stroke between 2007 and 2018 and had poststroke neuropsychological and neuropsychiatric assessment according to the Korean Vascular Cognitive Impairment Harmonization Standards: Neuropsychology Protocol (13,14), which also included the 30-item Geriatric Depression Scale (GDS-30). Patients underwent neuropsychological and neuropsychiatric assessment as part of clinical routine care, typically 3 months after stroke onset. Patients were excluded if they were unable to undergo these assessments owing to prior disabilities, including severe dysphasia, severe motor weakness, or impairment of hearing or vision, as determined by the attending physician. Baseline evaluation of demographics, vascular risk factors, and clinical characteristics, including stroke subtypes, severity of neurological symptoms, and functional status before index stroke, were obtained from the registry database. For the present study, 553 patients were selected based on the following criteria: 1) brain magnetic resonance imaging (MRI) showing the acute symptomatic infarct or infarcts on diffusion-weighted imaging (DWI) and/or fluid-attenuated inversion recovery (FLAIR); 2) successful infarct segmentation and registration (see Generation of Lesion Maps below); 3) no previous cortical infarcts, large subcortical infarcts, or intracerebral hemorrhages on MRI (see Generation of Lesion Maps); and 4) available GDS-30 assessment and clinical data on age, sex, and education. A flowchart of patient selection is provided in Figure 1.

Generation of Lesion Maps

Brain MRI, including DWI and FLAIR sequences, was performed with a 3T MRI scanner in the first week after stroke onset. The MRI protocol is provided in the Supplement. Lesion data were available from a previous project (15). In short, infarct segmentation and subsequent registration to the T1 1-mm MNI152 brain template (resolution 1 × 1 × 1 mm) (16) were performed in accordance with a previously published protocol (17). First, acute infarcts were manually segmented on DWI (n = 536; 97%) or FLAIR (n = 17; 3%) sequences using in-house developed software built in MeVisLab (MeVis Medical

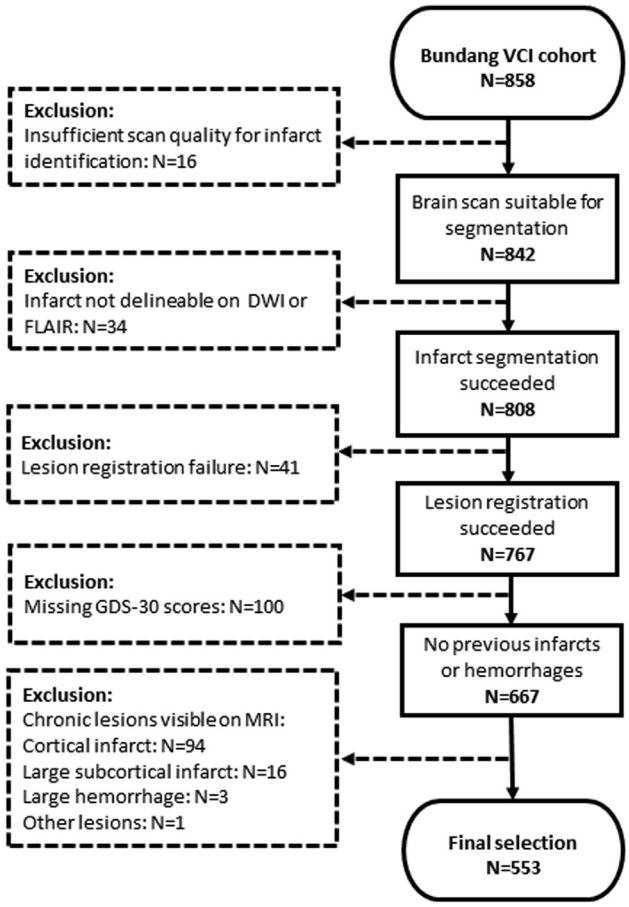

Figure 1. Flowchart of patient selection. DWI, diffusion-weighted imaging; FLAIR, fluid-attenuated inversion recovery; GDS-30, 30-item Geriatric Depression Scale; MRI, magnetic resonance imaging; VCI, Vascular Cognitive Impairment.

Solutions AG) (18). Apparent diffusion coefficient maps and T1 sequences were used as reference when available. Next, all scans and the corresponding lesion maps were transformed to MNI152 space with the RegLSM tool (https://github.com/Meta-VCI-Map/RegLSM). Quality checks of all registration results were performed by an experienced rater (NAW). Manual adaptations were made in case of minor registration errors (n = 255; 46%). The presence of chronic cortical infarcts (any size), large subcortical infarcts (>15 mm), and large intracerebral hemorrhages (>10 mm) was assessed by an experienced rater (NAW), and patients with any of these lesions were excluded from the current study.

Generation of Disconnectome Maps

Disconnectome maps were calculated using tractography data from the BCBtoolkit (19) MRI parameters and processing steps have been extensively described elsewhere (20). This approach uses connectome maps derived from DWI tractography data from 10 healthy control subjects (21) and uses lesion maps of patients as seed region for tractography to identify disconnected white matter fibers (19). In a previous validation study, data from these healthy control subjects generated disconnectome maps that matched their patient population (i.e., >70% shared variance) and ensured that the reliability of these disconnection maps did not decrease with increasing age (19).

We used the same lesion maps in MNI152 space as described in the previous step (see Generation of Lesion Maps above) to generate the disconnectome maps. Each patient's lesion map was registered to the native space of the healthy control subjects using affine and diffeomorphic deformations (22,23) and subsequently used as seed for the tractography in Trackvis (24). Tractographies from the lesions were transformed into visitation maps (25), binarized, and registered back to MNI152 space using the inverse of precedent deformations. Finally, a percentage overlap map was generated for each patient by summing the normalized visitation map of each healthy subject for each voxel in MNI152 space, indicating the probability of disconnection from 0% to 100%. Disconnectome maps were subsequently dichotomized (threshold ≥50%). Thus, the final disconnectome maps indicated whether an anatomical connection would normally exist in healthy individuals and consequently whether a voxel would become disconnected by the lesion.

Assessment of PSDS

Depressive symptoms were measured using a validated Korean version of the GDS-30 (26), which is a self-report questionnaire on depressive symptoms. Patients respond to a list of questions in "yes/no" format, with higher scores indicating a larger number of depressive symptoms (27). GDS-30 was administered within the first year after stroke by trained clinical neuropsychologists who were blinded to patients' clinical and neuroradiological profiles. No data on clinical history of depression or psychiatric disease were available.

Statistical Analyses

Outcome Measures. GDS-30 scores were used as a continuous measure to optimize statistical power for lesion-symptom mapping. GDS-30 scores were converted into standardized z scores and multiplied by −1, so that lower scores indicated more depressive symptoms. Correction for covariates was performed in 2 steps. First, z scores were corrected for age, sex, and years of education using linear regression. Second, we further took the influence of stroke severity, physical disability, and cognitive impairment into account because these were identified as the most consistent predictors of PSDS in a recent review (3). For this purpose, we performed additional correction for National Institutes of Health Stroke Scale (NIHSS) score, impairment of activities of daily living (ADL) according to the Korean Instrumental Activities of Daily Living, and presence of poststroke cognitive impairment (PSCI) based on multidomain neuropsychological assessment (definitions provided in the Supplement), all of which were administered on the same day as the GDS-30. Both corrected z scores (i.e., corrected for 3 and 6 factors, respectively) were analyzed separately as measures for PSDS in all support vector regression (SVR)–based analyses mentioned below.

Lesion-Symptom Mapping. We performed multivariable SVR-based analyses to determine the association between infarct location and PSDS. Two independent, hypothesis-free approaches were applied (28,29): voxel-based lesion-symptom mapping (SVR-VLSM) and region of interest (SVR-ROI). These methods offered complementary strengths: SVR-VLSM offers a much higher spatial resolution, while SVR-ROI takes the cumulative lesion burden within predefined brain regions into account.

SVR-VLSM was performed using SciPy 1.4.1 (Python; https://pypi.org/project/scipy/). Only voxels damaged in at least 5 patients were included in the analyses. A linear SVR model with feature selection was used, in accordance with previous studies (28,29). In the feature selection step, only voxels in which the presence of a lesion was univariately associated with depressive symptoms (two-sided t test, uncorrected $p < .05$) were selected to reduce noise. Next, parameter training of the linear SVR model was performed to determine the optimal regularization parameter (C) and epsilon to maximize prediction performance. Prediction performance was calculated for each combination of C and epsilon values by determining the mean Pearson correlation coefficient between the real and predicted z scores with fivefold cross-validations (optimal parameters in Table S2). Statistical inference was performed by shuffling the z scores and creating 5000 sets of pseudo weight coefficients, and the significance level of each voxel was calculated by counting the number of pseudo weights larger than the real weight in 5000 permutations. Directionality of effects was determined based on the weight coefficients, with positive weights indicating that the presence of an infarct was associated with more PSDS. Voxels with permutation-based $p < .05$ were treated as statistically significant. We corrected for total infarct volume by weighting the lesioned voxels in inverse proportion to the square root of total infarct volume before model training.

SVR-ROI was performed using MATLAB version R2018a (The MathWorks, Inc.). ROIs were defined using the Automated Anatomical Labeling atlas (119 ROIs) (30) and ICBM-DTI-81 white matter tract atlas (50 ROIs) (31,32) in MNI152 space

(16). Infarct volumes for each ROI were calculated in milliliters. Only ROIs damaged in at least 5 patients were included in the analyses. A linear SVR model with feature selection was used (33). In the feature selection step, ROIs with a univariate significant Pearson correlation ($p < .05$) between infarct volume and PSDS were selected. The parameter training and statistical inference of SVR-ROI corresponded with SVR-VLSM (optimal parameters in Table S3). ROIs with permutation-based $p < .05$ were treated as statistically significant. Of note, for SVR-ROI, total infarct volume correction was done differently than for SVR-VLSM: total infarct volume was included as a covariate alongside the ROI volumes during the feature selection step, meaning that it could be excluded if no univariate association was found.

Disconnection-Symptom Mapping. The association between anatomical disconnections and depressive symptoms was analyzed at the level of individual voxels using SVR-VLSM. The same SVR-VLSM approach was applied (see Lesion-Symptom Mapping above), but with two differences: disconnectome maps were entered as an independent variable instead of lesion maps, and we corrected for total disconnectome volume instead of total infarct volume. Voxels with permutation-based $p < .05$ were treated as statistically significant.

External Validation

To establish external validity and reproducibility, we determined whether the statistically significant ROIs identified in the SVR-ROI analysis were also associated with depressive symptoms in an independent study sample from the Hallym VCI cohort ($N = 459$) (details provided in the Supplement) (14). Study protocols and patient characteristics were comparable to the Bundang VCI cohort, and lesion data were collectively prepared in a previous study (15). In the Hallym VCI cohort, depressive symptoms were measured using a validated Korean version of the 15-item GDS (GDS-15) (34), which is a shorter version of the GDS-30. We followed the same data processing steps as for the Bundang VCI cohort; the only difference was the use of GDS-15 instead of GDS-30. Significant ROIs were selected from the SVR-ROI results ($p < .05$) and entered in separate multiple linear regression models, independently and after correction for age, sex, and education. This was done for both Bundang VCI and Hallym VCI datasets to allow for direct comparison. As a negative control, models were also built for 3 randomly selected ROIs that showed no association with PSDS in any of the analyses using GDS-30 in the main sample (note that contralateral ROIs were also excluded) and covered different areas of the brain (i.e., one left supratentorial, one right supratentorial, and one infratentorial ROI) to ascertain spatial independence. All ROI volumes underwent cube root transformation to meet the normality assumptions of multiple linear models. Standardized β (Stβ) values were calculated for each ROI.

Ethics Statement

Patient data were collected in accordance with study protocols approved by the Seoul National University Bundang Hospital Institutional Review Board and Hallym University Sacred Heart Hospital Institutional Review Board, with a waiver of patient consent because of the retrospective nature of the study and minimal risk to study participants. Use of data for the current study was also approved by the institutional review boards.

RESULTS

Study Population

Demographic and clinical characteristics of the 553 included patients are provided in Table 1. Mean (SD) age was 69 (11) years, 42% were female ($n = 233$), and median years of education was 9 (interquartile range [IQR] = 6–14 years). GDS-30 scores ranged from 0 to 30 (i.e., full range), with a median of 13 (IQR = 7–20). PSCI and ADL impairment occurred in 58% and 25% of patients, respectively, and median NIHSS score was 3 (IQR = 1–5). GDS-30 and cognitive assessments generally were done in the first 6 months after stroke, with a median time interval of 105 days (IQR = 11–168 days). Infarcts were generally small, with a median normalized volume of 3.3 mL (IQR = 1.1–15.1 mL).

Lesion-Symptom Mapping Results

Infarct distribution was symmetrical, and subcortical regions were more commonly damaged than cortical regions (Figure 2A). Brain coverage was relatively high: in the SVR-VLSM analyses, 52% of voxels of the MNI152 template (944,338/1,827,240 voxels) were included. Parts of the midbrain, temporal lobes, cerebellum, and anterior cerebral artery territory could not be included owing to infrequent involvement (i.e., damaged in <5 patients). In the SVR-ROI analyses, 167 of 169 ROIs were included.

SVR-VLSM showed that voxel clusters in the right amygdala, right pallidum, right corona radiata, right sagittal striatum, bilateral hippocampi, bilateral fornices, and left cingulum of the hippocampus were significantly associated with more PSDS (permutation-based $p < .05$), after correction for age, sex, education, total infarct volume, NIHSS score, ADL impairment, and PSCI (Figure 2B, C; Table S4).

SVR-ROI showed that infarct volumes in the right amygdala, right pallidum, and right hippocampus were significantly associated with more PSDS (permutation-based $p < .05$), after correction for age, sex, education, NIHSS score, ADL impairment, and PSCI (Figure 2D, E). Total infarct volume was not univariately associated with more PSDS, and therefore it was not included in the multivariable SVR-ROI models as a covariate. Statistically significant ROIs were subsequently entered in a univariable linear regression model (model 1 in Table 2), showing the strongest association between larger infarct volumes and more PSDS in the right amygdala (Stβ = −0.10) and right pallidum (Stβ = −0.09), followed by the hippocampus (Stβ = −0.07), also after correction for age, sex, and education (model 2 in Table 2).

All statistically significant voxels from SVR-VLSM and SVR-ROI analyses had positive weight coefficients and were therefore associated with more depressive symptoms. No infarct locations were significantly associated with fewer depressive symptoms.

Table 1. Demographic and Clinical Characteristics of Study Sample (*N* = 553)

Demographic and Clinical Characteristics	Value
Age, Years, Mean (SD)	69.0 (11.0)
Female, *n* (%)	233 (42%)
Years of Education, Median (IQR)	9 (6–14)
NIHSS Score at Admission, Median (IQR)	3 (1–5)
K-IADL Score, Median (IQR)	0.10 (0.00–0.42) (missing *n* = 4)
ADL Impairment (K-IADL Score >0.43), *n* (%)	137 (25%) (missing *n* = 4)
TOAST Classification for Ischemic Stroke Subtypes, *n* (%)	
Large artery atherosclerosis	200 (36%)
Cardioembolism	138 (25%)
Small vessel occlusion	120 (22%)
Other determined etiology	8 (1%)
Undetermined etiology	87 (16%)
Hand Preference, *n* (%)	(missing *n* = 2)
Right	534 (97%)
Left	6 (1%)
Ambidextrous	11 (2%)
Vascular Risk Factors, *n* (%)	
Hypertension	422 (76%)
Hyperlipidemia	135 (24%)
Current smoker	119 (22%)
Past smoker	113 (20%)
Diabetes mellitus	179 (32%)
Atrial fibrillation	84 (15%) (missing *n* = 27)
Neuropsychiatric and Cognitive Assessment	
Time interval between stroke onset and assessment, days, median (IQR), range	105 (11–168), 1–361
GDS-30 scores, median (IQR), range	13 (7–20), 0–30
Presence of poststroke cognitive impairment, *n* (%)	323 (58%) (missing *n* = 10)
Brain MRI	
Time interval between stroke onset and MRI, days, median (IQR), range	5 (4–6), 0–41
Total infarct volume, mL,[a] median (IQR), range	3.3 (1.1–15.1), 0.04–535.1

Missing data are noted following the respective variable, when appropriate. Valid percent is indicated in cases with missing data.

ADL, activities of daily living; IQR, interquartile range; K-IADL, Korean Instrumental Activities of Daily Living; MRI, magnetic resonance imaging; NIHSS, National Institutes of Health Stroke Scale; TOAST, Trial of Org 10172 in Acute Stroke Treatment.

[a]Normalized volumes after registration to the MNI152 template.

Disconnection-Symptom Mapping Results

Disconnections of nearly all supratentorial white matter fibers were included in the analyses, with a symmetrical distribution (Figure 3A). Disconnectome-based analyses with SVR-VLSM revealed that disconnections in the right parahippocampal white matter, right thalamus and pallidum, and right anterior thalamic radiation were significantly associated ($p < .05$) with more PSDS, after correction for age, sex, education, total disconnectome volume, NIHSS score, ADL impairment, and PSCI (Figure 3B). All statistically significant voxels from the disconnectome analysis had positive weight coefficients and were therefore associated with more depressive symptoms. No disconnection locations were significantly associated with fewer depressive symptoms.

External Validation

Demographic and clinical characteristics of the validation sample (Hallym VCI, $N = 459$) are shown in Table S5. Compared with the main sample (Bundang VCI, $N = 553$), the validation sample was younger (65 years vs. 69 years), had smaller infarcts (median volume: 1.9 mL vs. 3.3 mL), and had a lower occurrence of PSCI (44% vs. 58%) and ADL impairment (13% vs. 25%). Brain coverage was lower in the validation sample, particularly in bilateral temporal and occipital lobes, owing to the smaller infarcts and smaller sample size (Figure S2). Based on the SVR-ROI results (Figure 2E), the right amygdala, right hippocampus, and right pallidum ROIs were selected for the external validation (Table 2).

In the validation sample, regional infarct volumes in the right amygdala ($St\beta = -0.15$, $p = .001$) and right pallidum ($St\beta = -0.14$, $p = .002$) were significantly associated with more PSDS, with slightly larger effect sizes than in the main sample ($St\beta = -0.11$ and -0.09, respectively). By contrast, the association with the right hippocampus was not confirmed ($St\beta = -0.03$, $p = .5$). ROIs randomly selected as negative controls were not associated with PSDS in the validation sample (Table 2).

DISCUSSION

In this large-scale lesion-symptom mapping study, we newly identified the right amygdala as an infarct location associated with PSDS and further pinpointed the right pallidum as a key location within the basal ganglia. This finding was replicated in an independent cohort. Furthermore, we showed that structural disconnections located in right thalamocortical and parahippocampal white matter were associated with PSDS. This converging evidence demonstrates that infarcts and resulting structural disconnections located in right frontal cortico-thalamic and limbic circuits are related to PSDS.

The relationship between infarct location and PSDS has been extensively studied, yet previous findings varied widely. Early studies were limited by technical constraints and could consider only relatively crude spatial characteristics, such as hemispheric lateralization or lobar involvement (5). Recent lesion-symptom mapping studies provided a higher spatial resolution, but they still lacked consistent evidence, likely owing to modest sample sizes and subsequent limited lesion coverage and inclusion of mixed pathologies. In our large homogeneous sample, we achieved high brain coverage [i.e., 52% compared with <25% in most monocenter lesion-symptom mapping studies (28)] and thereby created the most comprehensive picture of strategic infarct locations for PSDS to date.

A recent systematic review and meta-analysis found that infarcts in the basal ganglia were significantly associated with PSDS (4). We confirm and extend these findings by pinpointing the pallidum and more specifically the ventral pallidum (i.e.,

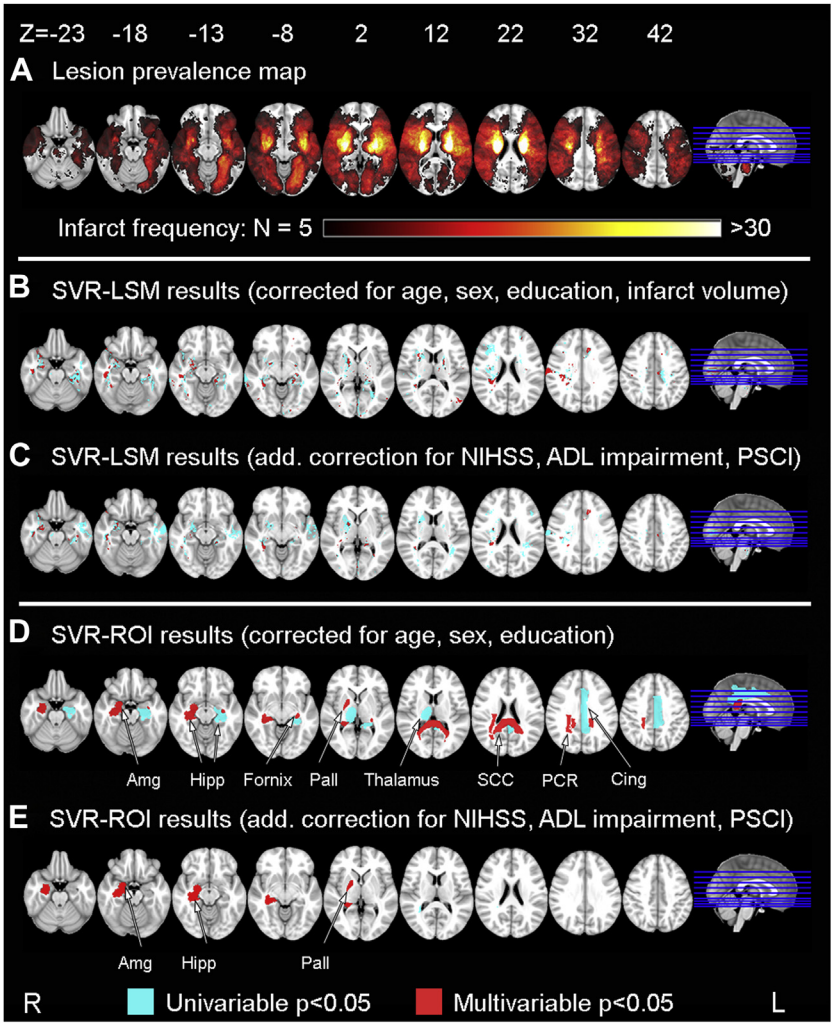

Figure 2. Lesion prevalence map and lesion-symptom mapping results. Results are depicted on the MNI152 T1 1 mm template. **(A)** Infarct prevalence map showing voxels that are damaged in ≥5 patients (N = 553). Only colored voxels were included in subsequent analyses. **(B, C)** Results of support vector regression voxel-based lesion-symptom mapping (SVR-VLSM). First, feature selection was performed using univariable VLSM (two-sample t test; $p < .05$). Next, linear SVR-VLSM was performed on these selected voxels (shown in red and cyan). Significant voxels from the SVR LSM analysis are shown in red ($p < .05$ based on 5000 permutations); feature-selected but nonsignificant voxels are shown in cyan. **(D, E)** Results of SVR region of interest (ROI). ROIs were defined by the Automated Anatomical Labeling gray matter atlas and ICBM-DTI-81 white matter tract atlas in MNI152 space. First, feature selection was performed using regional infarct volumes and total infarct volume (Pearson correlation; $p < .05$). Note that total infarct volume was not selected in this step. Next, linear SVR-ROI was performed on these selected ROIs (shown in red and cyan). Significant ROIs from the SVR-ROI analysis are shown in red ($p < .05$ based on 5000 permutations); feature-selected but nonsignificant voxels are shown in cyan. In all significant voxels from SVR-LSM and SVR-ROI, the presence of an infarct was associated with more poststroke depressive symptoms; none of the significant voxels were associated with fewer poststroke depressive symptoms. Add., additional; ADL, activities of daily living; Amg, amygdala; Cing, cingulate gyrus; Hipp, hippocampus; L, left; NIHSS, National Institutes of Health Stroke Scale; Pall, pallidum; PCR, posterior corona radiata; PSCI, poststroke cognitive impairment; R, right; SCC, splenium of the corpus callosum.

based on the VLSM analyses) as a key anatomical structure within the basal ganglia. This increased anatomical detail is important because the basal ganglia consist of a multitude of structures and projections, within which the ventral pallidum is a core component of the limbic loop (35). Furthermore, we identified the right amygdala as a strategic infarct location, which has been suggested only once before in a study in 68 patients with stroke (36). This limited prior evidence on the amygdala might be due to its infrequent involvement and subsequent limited statistical power in smaller studies, considering that the amygdala is supplied by the anterior choroidal artery (37). Restricted anterior choroidal artery infarcts (i.e., left or right) account for only 8% of patients with acute ischemic stroke (38). Of note, in our sample the right amygdala was rarely damaged (n = 37; 6.7%) and in most cases as part of a larger middle cerebral artery infarct, though focal infarcts to the anterior choroidal artery territory also occurred (illustrated in Figure S3). An important strength of our study is that we externally validated the relevance of these locations in an independent dataset. Despite the use of a different version of the GDS and differences in cohort characteristics (i.e., age, infarct size, and presence of functional impairment), the right amygdala and pallidum showed comparable associations with PSDS in both stroke cohorts. This demonstrates the robustness and generalizability of our findings.

Recent evidence suggests that PSDS can result from interruptions of functional brain networks caused by infarcts (9). Our complementary analytical approaches provide an integrated perspective, showing that both infarct location and structural disconnections are important. Our voxel-based analyses showed a clear pattern of involvement of voxel clusters in limbic system structures, including the amygdala and ventral pallidum, but also the hippocampus, fornix, cingulate gyrus, and cingulum of the hippocampus. Meanwhile, the disconnectome-based analysis showed specific involvement of tracts connecting the right frontal cortex to the pallidum and thalamus and from the thalamus to the parahippocampal white matter. Taking these findings together, the right limbic and frontal cortico-basal ganglia-thalamic circuits consistently

Table 2. External Validation of Identified Regions of Interest in an Independent Dataset

	Bundang VCI (*N* = 553), Original Sample			Hallym VCI (*N* = 459), Validation Sample		
	Standardized β for ROI Volume	*p* Value	Patients With ROI Damaged (*n*)	Standardized β for ROI Volume	*p* Value	Patients With ROI Damaged (*n*)
Model 1: ROI Volume Only						
Right amygdala	−0.10	.024	37	−0.16	.371	32
Right hippocampus	−0.07	.082	57	−0.04	.001	38
Right pallidum	−0.09	.037	65	−0.13	.004	67
Left insula (negative control)[a]	0.01	.909	128	−0.02	.618	85
Middle cerebellar peduncle (negative control)[a]	0.01	.901	101	0.01	.759	77
Right middle occipital gyrus (negative control)[a]	−0.03	.544	56	−0.09	.062	39
Model 2: Age, Sex, Education, and ROI Volume						
Right amygdala	−0.11	.007	37	−0.15	.001	32
Right hippocampus	−0.08	.043	57	−0.03	.478	38
Right pallidum	−0.09	.023	65	−0.14	.002	67
Left insula (negative control)[a]	0.01	.800	128	−0.03	.478	85
Middle cerebellar peduncle (negative control)[a]	0.01	.847	101	0.01	.821	77
Right middle occipital gyrus (negative control)[a]	−0.03	.480	56	−0.07	.113	39

Linear regression was used to determine whether ROI volumes of the significant regions from the support vector regression ROI analyses (Figure 2E) were associated with poststroke depressive symptoms in an independent dataset. Poststroke depressive symptoms were measured with the 30-item Geriatric Depression Scale (GDS) in the Bundang VCI cohort and the 15-item GDS in the Hallym VCI cohort. ROIs were defined by the Automated Anatomical Labeling gray matter atlas and ICBM-DTI-81 white matter tract atlas in MNI152 space. ROI volumes underwent cube root transformation before statistical analyses. Two models were built. In model 1, each ROI volume was entered by itself as an independent variable, and GDS scores (i.e., converted into *z* scores and multiplied by −1, so that lower scores indicated more poststroke depressive symptoms) were entered as a dependent variable. In model 2, each ROI volume was entered together with age, sex, and level of education as independent variables, and GDS scores were entered as a dependent variable. Standardized β values and *p* values are reported for both the original sample and the validation sample to allow for comparison.

ROI, region of interest; VCI, Vascular Cognitive Impairment.

[a]Models were also built for 3 ROIs that were not associated with poststroke depressive symptoms in the Bundang VCI cohort to strengthen the generalizability of the findings.

emerge as key brain networks, in which both direct damage to key brain structures and disruption of connecting pathways are linked to PSDS.

The pathophysiology of PSDS is complex and involves a combination of biological and psychosocial factors (3). Our findings strengthen the notion that lesion location is a contributing biological factor and suggest a central role of the limbic system. This is in line with evidence from studies on depression as a primary psychiatric disorder. Decreased amygdala and hippocampus volumes were found in patients with depression, and functional MRI and positron emission tomography studies have reported changes in metabolism or activity in the amygdala and hippocampus (39). Diffusion tensor imaging–based studies have reported structural alterations to frontostriatothalamic white matter tracts in patients with depression (40). Meanwhile, white matter hyperintensities are also thought to contribute to depressive symptoms in elderly people through disruption of structural brain networks (i.e., the vascular depression hypothesis) (41,42). White matter hyperintensities located in (pre)frontal and temporal regions have been associated with depressive symptoms (43–46), which aligns with locations identified in our disconnectome-based analyses. This suggests that vascular damage to the frontolimbic circuits represents a common mechanism of depressive symptoms in cerebral small vessel disease and acute ischemic stroke (5).

Poststroke physical and cognitive deficits have also been linked to PSDS, indirectly suggesting that PSDS may be a psychological reaction to these deficits (3,47). Our results were independent of measures of stroke severity, physical disability, and cognitive impairment, which supports the notion of a direct effect of infarcts on the depressive symptoms.

A notable observation is that most of the infarct locations associated with PSDS were located in the right hemisphere, even though our lesion coverage was nearly symmetrical. The impact of lesion laterality in PSDS has been a topic of extensive discussion, but no clear pattern has been found. A recent meta-analysis found no association with laterality in 60 studies, in neither the pooled analysis nor subgroup analyses stratified by study phase (i.e., acute, subacute, and chronic) (4). Evidence on laterality from other neuroimaging research on depression (e.g., electroencephalography, functional MRI, positron emission tomography) is also inconclusive (48). Our results should therefore not be interpreted as specific to the right hemisphere, but rather to highlight the importance of specific brain structures and networks.

Some limitations to our study must be noted. First, the GDS-30 was designed as a screening tool. While the questionnaire allows for quantification of the number of depressive symptoms, it cannot establish a formal diagnosis of poststroke depression. A formal diagnosis might be more relevant from a clinical perspective but would require elaborate evaluation by a

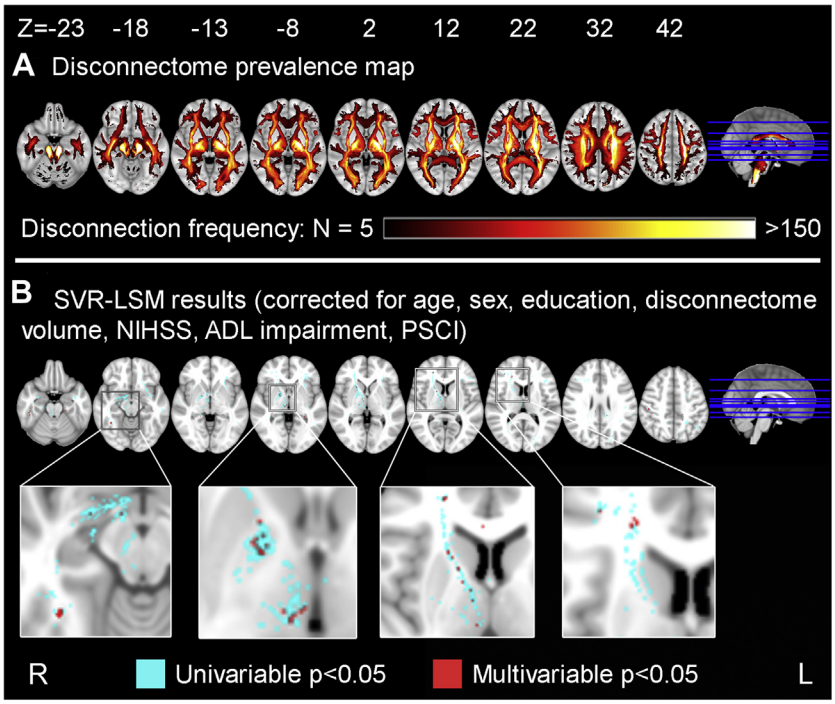

Figure 3. Structural disconnection prevalence map and disconnection-symptom mapping results. Results are depicted on the MNI152 T1 1 mm template. **(A)** Structural disconnection prevalence map showing voxels that are affected in ≥5 patients (total $N = 553$). Only colored voxels were included in subsequent analyses. **(B)** Results of support vector regression lesion-symptom mapping (SVR-LSM). Note that this method is the same as for the infarct location-based analysis (Figure 2B, C), but using the map of disconnections caused by the infarct as determinant instead of the infarct itself. First, feature selection was performed using univariable voxel-based lesion-symptom mapping (two-sample *t* test; $p < .05$). Next, linear SVR-LSM was performed on these selected voxels (shown in red and cyan). Significant voxels from the SVR-LSM analysis are shown in red ($p < .05$ based on 5000 permutations); feature-selected but nonsignificant voxels are shown in cyan. In all significant voxels from the SVR-LSM and SVR region-of-interest analyses, the presence of an infarct was associated with more poststroke depressive symptoms; none of the significant voxels were associated with fewer poststroke depressive symptoms. ADL, activities of daily living; L, left; NIHSS, National Institutes of Health Stroke Scale; PSCI, poststroke cognitive impairment; R, right.

psychiatrist, which might prove difficult to achieve in large-scale stroke studies. Second, information on clinical history of depression was not collected; therefore, we could not take potential influence of depressive symptoms before stroke into account. Third, our analysis of structural disconnections was based on a brain connectivity template and not the actual brain connectivity of individual patients; therefore, patient-specific variability in brain connectivity might not be fully accounted for. Fourth, the time interval between stroke onset and GDS assessment was relatively wide, ranging from 1 to 361 days. Brain plasticity and functional recovery can occur after stroke, and the degree of recovery may depend on which brain region is damaged (49). However, little is known about the natural trajectory of PSDS, and the ideal timing for assessment is unclear, making this factor difficult to take into account (3). Fifth, owing to the retrospective nature of our study and selection criteria, prevalence of PSDS in the study group might not reflect the prevalence in the overall stroke population. Finally, although we excluded patients with chronic infarcts and hemorrhages to reduce the effect of prior vascular lesions on the lesion-deficit associations, we could not evaluate the potential influence of white matter hyperintensities owing to technical constraints. Considering the known impact of white matter hyperintensities on depressive symptoms in other populations, this should be evaluated in future studies.

Our study contributes to the knowledge of the pathophysiology of poststroke depression by highlighting the involvement of specific brain structures and connections. As a next step, the value of strategic infarct location as a prognostic imaging marker could be assessed using predictive modeling, similar to a recent study on PSCI prediction (50). If successful, this could facilitate early identification of patients at risk of developing PSDS, permit more timely intervention and treatment of these debilitating symptoms, and thereby lower the burden on both patients and caregivers.

ACKNOWLEDGMENTS AND DISCLOSURES

This work was supported by a Vici grant from ZonMw, The Netherlands Organisation for Health Research and Development (Grant No. 918.16.616 [to GJB]), and a Young Talent Fellowship from the UMC Utrecht Brain Center (to JMB).

We thank Gözdem Arikan and Angelina Kancheva for their help with the infarct segmentations and Jaeseol Park and Eunbin Ko for their help in organizing the clinical data.

Data from this article were presented at the 7th European Stroke Conference, September 1–3, 2021 (virtual). A previous version of this article was published as a preprint on bioRxiv: https://doi.org/10.1101/2021.05.05.442398.

The authors report no biomedical financial interests or potential conflicts of interest.

ARTICLE INFORMATION

From the Department of Neurology and Neurosurgery (NAW, JS, GJB, JMB), UMC Utrecht Brain Center, University Medical Center Utrecht; Image Sciences Institute (HJK), University Medical Center Utrecht, Utrecht, The Netherlands; Department of Neurology (J-SL), Asan Medical Center, Seoul; Department of Neurology (YK, B-CL, K-HY), Hallym University Sacred Heart Hospital, Hallym Neurological Institute, College of Medicine, Hallym University, Anyang; Department of Psychology (YK), Hallym University, Chuncheon; and Department of Neurology (BJK, K-JL, H-JB), Seoul National University Bundang Hospital, Seoul National University College of Medicine, Seongnam, Republic of Korea.

Hee-Joon Bae and J. Matthijs Biesbroek contributed equally to this work.

Address correspondence to Nick A. Weaver, M.D., at n.a.weaver@umcutrecht.nl.

Received Jul 12, 2021; revised Aug 11, 2021; accepted Sep 8, 2021.

Supplementary material cited in this article is available online at https://doi.org/10.1016/j.bpsc.2021.09.002.

REFERENCES

1. Hackett ML, Pickles K (2014): Part I: Frequency of depression after stroke: An updated systematic review and meta-analysis of observational studies. Int J Stroke 9:1017–1025.
2. Kutlubaev MA, Hackett ML (2014): Part II: Predictors of depression after stroke and impact of depression on stroke outcome: An updated systematic review of observational studies. Int J Stroke 9:1026–1036.
3. Towfighi A, Ovbiagele B, El Husseini N, Hackett ML, Jorge RE, Kissela BM, *et al.* (2017): Poststroke Depression: A Scientific Statement for Healthcare Professionals from the American Heart Association/American Stroke Association. Stroke 48:e30–e43.
4. Douven E, Köhler S, Rodriguez MMF, Staals J, Verhey FRJ, Aalten P (2017): Imaging markers of post-stroke depression and apathy: A systematic review and meta-analysis. Neuropsychol Rev 27:202–219.
5. Nickel A, Thomalla G (2017): Post-stroke depression: Impact of lesion location and methodological limitations-a topical review. Front Neurol 8:498.
6. Gozzi SA, Wood AG, Chen J, Vaddadi K, Phan TG (2014): Imaging predictors of poststroke depression: Methodological factors in voxel-based analysis. BMJ Open 4:4948.
7. Grajny K, Pyata H, Spiegel K, Lacey EH, Xing S, Brophy C, Turkeltaub PE (2016): Depression symptoms in chronic left hemisphere stroke are related to dorsolateral prefrontal cortex damage. J Neuropsychiatry Clin Neurosci 28:292–298.
8. Kim NY, Lee SC, Shin JC, Park JE, Kim YW (2017): Voxel-based lesion symptom mapping analysis of depressive mood in patients with isolated cerebellar stroke: A pilot study. Neuroimage Clin 13:39–45.
9. Padmanabhan JL, Cooke D, Joutsa J, Siddiqi SH, Ferguson M, Darby RR, *et al.* (2019): A human depression circuit derived from focal brain lesions. Biol Psychiatry 86:749–758.
10. Sagnier S, Munsch F, Bigourdan A, Debruxelles S, Poli M, Renou P, *et al.* (2019): The influence of stroke location on cognitive and mood impairment. A voxel-based lesion-symptom mapping study. J Stroke Cerebrovasc Dis 28:1236–1242.
11. Klingbeil J, Brandt ML, Wawrzyniak M, Stockert A, Schneider HR, Baum P, *et al.* (2021): Association of lesion location and depressive symptoms poststroke. Stroke 52:830–837.
12. Kim BJ, Park JM, Kang K, Lee SJ, Ko Y, Kim JG, *et al.* (2015): Case characteristics, hyperacute treatment, and outcome information from the clinical research center for stroke-fifth division registry in South Korea. J Stroke 17:38–53.
13. Lim JS, Noh M, Kim BJ, Han MK, Kim S, Jang MS, *et al.* (2017): A methodological perspective on the longitudinal cognitive change after stroke. Dement Geriatr Cogn Disord 44:311–319.
14. Lim J, Kim N, Jang MU, Han M, Kim S, Baek MJ, *et al.* (2014): Cortical hubs and subcortical cholinergic pathways as neural substrates of poststroke dementia. Stroke 45:1069–1076.
15. Weaver NA, Kancheva AK, Lim JS, Biesbroek JM, Wajer IMH, Kang Y, *et al.* (2021): Post-stroke cognitive impairment on the Mini-Mental State Examination primarily relates to left middle cerebral artery infarcts. Int J Stroke 16:981–989.
16. Fonov V, Evans AC, Botteron K, Almli CR, McKinstry RC, Collins DL, Brain Development Cooperative Group (2011): Unbiased average age-appropriate atlases for pediatric studies. Neuroimage 54:313–327.
17. Biesbroek JM, Kuijf HJ, Weaver NA, Zhao L, Duering M, Biessels GJ (2019): Brain infarct segmentation and registration on MRI or CT for lesion-symptom mapping. J Vis Exp. 10.3791/59653.
18. Ritter F, Boskamp T, Homeyer A, Laue H, Schwier M, Link F, Peitgen H (2011): Medical image analysis. IEEE Pulse 2:60–70.
19. Foulon C, Cerliani L, Kinkingnéhun S, Levy R, Rosso C, Urbanski M, *et al.* (2018): Advanced lesion symptom mapping analyses and implementation as BCBtoolkit. GigaScience 7:1–17.
20. Thiebaut de Schotten M, Dell'Acqua F, Forkel SJ, Simmons A, Vergani F, Murphy DGM, Catani M (2011): A lateralized brain network for visuospatial attention. Nat Neurosci 14:1245–1246.
21. Rojkova K, Volle E, Urbanski M, Humbert F, Dell'Acqua F, Thiebaut de Schotten M (2016): Atlasing the frontal lobe connections and their variability due to age and education: a spherical deconvolution tractography study. Brain Struct Funct 221:1751–1766.
22. Klein A, Ghosh SS, Avants B, Yeo B, Fischl B, Ardekani B, *et al.* (2010): Evaluation of volume-based and surface-based brain image registration methods. Neuroimage 51:214–220.
23. Avants BB, Tustison NJ, Song G, Cook PA, Klein A, Gee JC (2011): A reproducible evaluation of ANTs similarity metric performance in brain image registration. Neuroimage 54:2033–2044.
24. Wang R, Benner T, Sorensen AG, Wedeen VJ (2007): Diffusion toolkit: A software package for diffusion imaging data processing and tractography. Proc Intl Soc Mag Reson Med 15:3720.
25. Thiebaut de Schotten M, Ffytche DH, Bizzi A, Dell'Acqua F, Allin M, Walshe M, *et al.* (2011): Atlasing location, asymmetry and inter-subject variability of white matter tracts in the human brain with MR diffusion tractography. Neuroimage 54:49–59.
26. Jung IK, Kwak DI, Shin DK, Lee MS, Lee HS, Kim JY (1997): A reliability and validity study of Geriatric Depression Scale. J Korean Neuropsychiatr Assoc 36:103–112.
27. Yesavage JA, Brink TL, Rose TL, Lum O, Huang V, Adey M, Leirer VO (1982): Development and validation of a geriatric depression screening scale: A preliminary report. J Psychiatr Res 17:37–49.
28. Weaver NA, Zhao L, Biesbroek JM, Kuijf HJ, Aben HP, Bae HJ, *et al.* (2019): The Meta VCI Map consortium for meta-analyses on strategic lesion locations for vascular cognitive impairment using lesion-symptom mapping: Design and multicenter pilot study. Alzheimers Dement (Amst) 11:310–326.
29. Zhao L, Biesbroek JM, Shi L, Liu W, Kuijf HJ, Chu WC, *et al.* (2018): Strategic infarct location for post-stroke cognitive impairment: A multivariate lesion-symptom mapping study. J Cereb Blood Flow Metab 38:1299–1311.
30. Tzourio-Mazoyer N, Landeau B, Papathanassiou D, Crivello F, Etard O, Delcroix N, *et al.* (2002): Automated anatomical labeling of activations in SPM using a macroscopic anatomical parcellation of the MNI MRI single-subject brain. Neuroimage 15:273–289.
31. Mori S, Oishi K, Jiang H, Jiang L, Li X, Akhter K, *et al.* (2008): Stereotaxic white matter atlas based on diffusion tensor imaging in an ICBM template. Neuroimage 40:570–582.
32. Oishi K, Zilles K, Amunts K, Faria A, Jiang H, Li X, *et al.* (2008): Human brain white matter atlas: Identification and assignment of common anatomical structures in superficial white matter. Neuroimage 43:447–457.
33. Yourganov G, Fridriksson J, Rorden C, Gleichgerrcht E, Bonilha L (2016): Multivariate connectome-based symptom mapping in post-stroke patients: Networks supporting language and speech. J Neurosci 36:6668–6679.
34. Cho MJ, Bae JN, Suh GH, Hahm BJ, Kim JK, Lee DW, Kang MH (1999): Validation of Geriatric Depression Scale, Korean Version(GDS) in the assessment of DSM-III-R major depression. J Korean Neuropsychiatr Assoc 38:48–63.
35. Smith KS, Tindell AJ, Aldridge JW, Berridge KC (2009): Ventral pallidum roles in reward and motivation. Behav Brain Res 196:155–167.
36. Terroni L, Amaro E, Iosifescu DV, Tinone G, Sato JR, Leite CC, *et al.* (2011): Stroke lesion in cortical neural circuits and post-stroke incidence of major depressive episode: A 4-month prospective study. World J Biol Psychiatry 12:539–548.
37. Kiernan JA (2012): Anatomy of the temporal lobe. Epilepsy Res Treat 2012:176157.
38. Ois A, Cuadrado-Godia E, Solano A, Perich-Alsina X, Roquer J (2009): Acute ischemic stroke in anterior choroidal artery territory. J Neurol Sci 281:80–84.
39. Pandya M, Altinay M, Malone DA, Anand A (2012): Where in the brain is depression? Curr Psychiatry Rep 14:634–642.
40. Chen G, Hu X, Li L, Huang X, Lui S, Kuang W, *et al.* (2016): Disorganization of white matter architecture in major depressive disorder: A

meta-analysis of diffusion tensor imaging with tract-based spatial statistics. Sci Rep 6:21825.

41. Alexopoulos GS, Meyers BS, Young RC, Campbell S, Silbersweig D, Charlson M (1997): "Vascular depression" hypothesis. Arch Gen Psychiatry 54:915–922.
42. Sneed JR, Culang-Reinlieb ME (2011): The vascular depression hypothesis: An update. Am J Geriatr Psychiatry 19:99–103.
43. Leeuwis AE, Weaver NA, Biesbroek JM, Exalto LG, Kuijf HJ, Hooghiemstra AM, *et al.* (2019): Impact of white matter hyperintensity location on depressive symptoms in memory-clinic patients: A lesion-symptom mapping study. J Psychiatry Neurosci 44:E1–E10.
44. Soennesyn H, Oppedal K, Greve OJ, Fritze F, Auestad BH, Nore SP, *et al.* (2012): White matter hyperintensities and the course of depressive symptoms in elderly people with mild dementia. Dement Geriatr Cogn Dis Extra 2:97–111.
45. Dalby RB, Frandsen J, Chakravarty MM, Ahdidan J, Sørensen L, Rosenberg R, *et al.* (2010): Depression severity is correlated to the integrity of white matter fiber tracts in late-onset major depression. Psychiatry Res Neuroimaging 184:38–48.
46. Sheline YI, Price JL, Vaishnavi SN, Mintun MA, Barch DM, Epstein AA, *et al.* (2008): Regional white matter hyperintensity burden in automated segmentation distinguishes late-life depressed subjects from comparison subjects matched for vascular risk factors. Am J Psychiatry 165:524–532.
47. Nys GMS, Van Zandvoort MJE, Van Der Worp HB, De Haan EHF, De Kort PLM, Kappelle LJ (2005): Early depressive symptoms after stroke: Neuropsychological correlates and lesion characteristics. J Neurol Sci 228:27–33.
48. Bruder GE, Stewart JW, McGrath PJ (2017): Right brain, left brain in depressive disorders: Clinical and theoretical implications of behavioral, electrophysiological and neuroimaging findings. Neurosci Biobehav Rev 78:178–191.
49. Karnath HO, Rennig J, Johannsen L, Rorden C (2011): The anatomy underlying acute versus chronic spatial neglect: A longitudinal study. Brain 134(Pt 3):903–912.
50. Weaver NA, Kuijf HJ, Aben HP, Abrigo J, Bae HJ, Barbay M, *et al.* (2021): Strategic infarct locations for post-stroke cognitive impairment: A pooled analysis of individual patient data from 12 acute ischaemic stroke cohorts. Lancet Neurol 20:448–459.